

Multiscale modeling of the competition between intergranular and transgranular ductile fracture in Al alloys

F. Scheyvaerts¹, P.R. Onck², Y. Bréchet³, T. Pardoen¹

¹*Institute of mechanical, materials and civil engineering, Université catholique de Louvain, Place Sainte Barbe 2, B-1348 Louvain-la-Neuve, Belgium*

²*Micromechanics of Materials, Zernike Institute for Advanced Materials, University of Groningen, Nijenborgh 4, 9747 AG Groningen, The Netherlands*

³*SIMAP-ENSEEG, Domaine Universitaire de Grenoble BP75, F-38402, Saint Martin d'Heres, France*

Abstract

The competition between intergranular and transgranular ductile fracture in Al alloys with precipitate free zones is investigated using a multiscale FE based approach. The solid is represented by discrete grains. Each grain is made of harder interior core and softer grain boundary layers, each region being discretized with many elements and represented by different hardening and damage related parameters. The material behaviour is given by an advanced micromechanical damage model for the transition to the smallest scale. This model relies on the extension of the Gurson model by Gologanu while introducing a new void rotation law and a new generalized void coalescence model. Homogenous biaxial loading, tensile testing with necking and crack propagation from a precrack are simulated to investigate the relationships between the hardening law, microstructure parameters, stress state, fracture mechanisms and fracture resistance expressed by a fracture strain or a J_R curve.

1. Introduction

Many Al, Ti, Ni or Fe-based metallic alloys involve micron or submicron thick layers surrounding Grain Boundaries (GB) with a microstructure different from the bulk of the grain, e.g. [1-3]. In several circumstances, the GB layers are softer than the grain interior, due to a lack of nanoscale hardening precipitates. The presence of these soft zones favors the occurrence of a low toughness intergranular fracture. A classical example is given by the Al alloys of the 7xxx series with important implications for instance in aeronautical applications.

As shown in Fig. 1, ductile damage occurs both inside the grains and within the GB layers through the nucleation of voids by cracking or decohesion of large second phases, void growth and coalescence. The goal of this study is to investigate the influence of the parameters describing the microstructure and of the flow properties on the cracking resistance and preferential crack path using a multiscale approach. Improving the understanding of the competition between intergranular and transgranular failure will support the optimization of the

material microstructure. In this paper we will use and extend advanced micromechanics-based damage models in order to allow a realistic treatment of void growth and coalescence under various loading conditions, involving low and large stress triaxiality as well as significant shear strains, various strain hardening responses and microstructural features (e.g. shape, volume fraction, and distribution of second phase particles). The specific application is on 7xxx Al alloys, although the approach, and several results, are valid for other heterogeneous alloys as well.

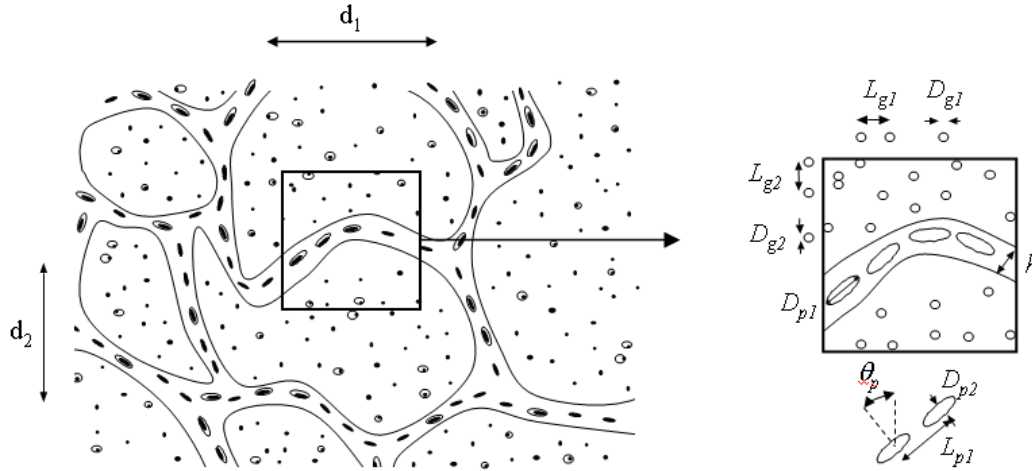


Fig. 1. Description of (a) the microstructure and failure mechanisms, and of (b) the idealised microstructure.

2. Description of the models and numerical procedures

The fracture mechanisms are investigated at different scales and with various levels of sophistication, using different representations of the microstructure and employing the FE method. The different models are shown in Fig. 2.

Model 1 – Bilayer model – Fig. 2a. This model describes the response at the grain level by a soft zone sandwiched between two hard grains, essentially assuming that the competition in the damage and fracture evolution is controlled by the GB layers perpendicular to the main loading direction. This simple representation of the microstructure has been addressed in details in a former study [4].

Model 2 – Single grain model – Fig. 2b. This model improves Model 1 by a more realistic description of the grain involving a hexagonal shape (which can be equiaxed or not) and GB layers inclined with respect to the main loading direction. Periodic boundary conditions are enforced. Fig. 2b shows the unit cell which, owing to the symmetries, consist of only a portion of the grain.

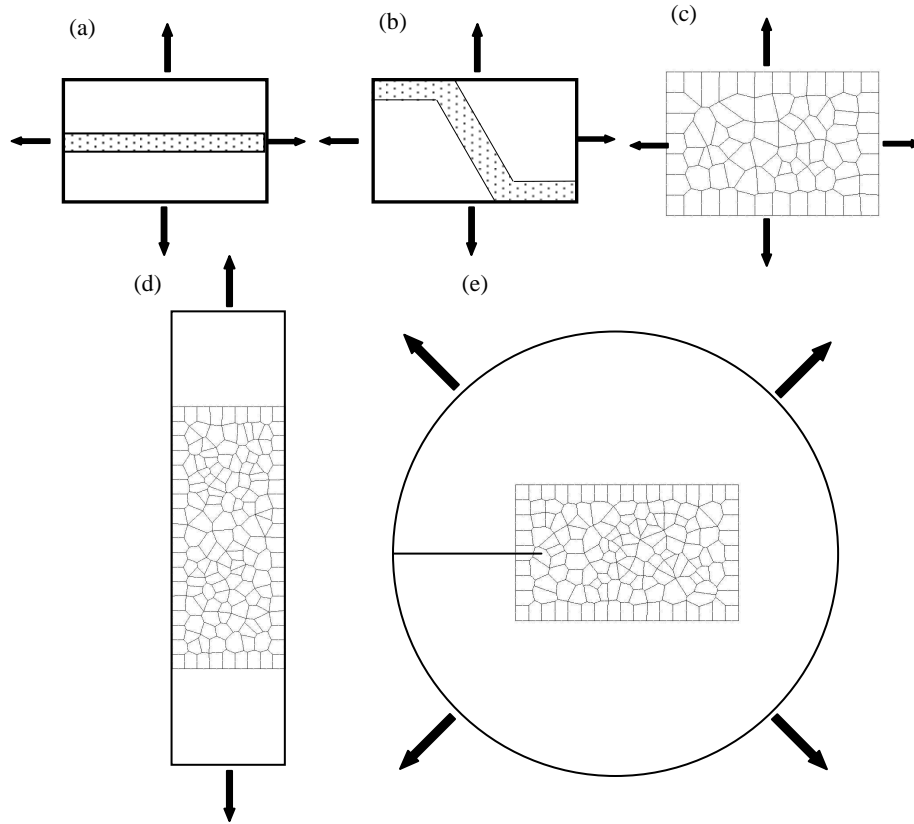


Fig. 2. Five models to simulate the damage evolution and cracking resistance of polycrystalline alloys involving soft grain boundary layers and hard grain interiors.

Model 3 – Multi-grain model under homogenous loading conditions – Fig. 2c. Compared to Model 2, the multi-grain representation provides statistical results, by dealing with more realistic grain shape and size distributions, and allows the coexistence of both failure modes and the simulation of complex crack paths.

Model 4 – Multigrain tensile test sample – Fig. 2d. The multi-grain window is embedded into a tensile test sample, in order to simulate a test involving necking, in order to generate realistic information about ductility, fracture surface orientation, and crack path that can be compared to experimental results.

Model 5 – Small scale yielding (SSY) multigrain model – Fig. 2e. The multigrain window is embedded into a large domain subjected to a K-field with a pre-existing macro-crack. The domain is large enough to enforce small scale yielding conditions and to generate constraint-independent J_R curves.

For each of these models, the GB layers (shown in Fig. 2a,b, but not in c,d,e) are meshed with one or two elements over the thickness. The grain interiors are finely meshed, especially in Models 1 and 2. The multigrain box is constructed based on a Voronoi tessellation procedure. The models are all 2D plane strain.

The response of the grain interior and GB layer is described by the same constitutive model. This model combines the extension by Gologanu *et al.* [5] of the Gurson model [6] to a spheroidal void shape, a void rotation law borrowed from Ponte-Castañeda's work [7], an extension of Thomason's void coalescence condition [8] to general loading conditions, and a new micromechanical model for the final drop of the load carrying capacity [9]. The internal variables of the model are the six components of the stress tensor, void volume fraction, void shape parameter, void orientation and relative void spacing. Evolution laws are given for each of them. The detailed description of this model and of its implementation in an in-house FE code within a finite strain setting is given elsewhere (see earlier work in [10] and new extensions in [11]), in order to focus this paper on selected key physical mechanisms.

The hardening law for the material in the grain interior and in the GB layer is given by a power law description:

$$\frac{\sigma}{\sigma_0} = \frac{E\varepsilon}{\sigma_0} \quad \text{when } \sigma < \sigma_0, \quad (1)$$

$$\frac{\sigma}{\sigma_0} = \left(1 + \frac{E\varepsilon^n}{\sigma_0} \right) \quad \text{when } \sigma > \sigma_0 \quad (2)$$

where E is the Young's modulus, σ_0 is the yield stress, and n is the strain-hardening exponent. The material parameters used in all calculations reported in the present paper are typical for 7xxx Al alloys ([1]), see Table 1 with definition. A subscript "g" (resp. "p") is used when referring to the grain interior (resp. for the GB layer). The relative thickness of the GB layer with respect to the grain size, R_0 , is equal to 0.0525, the grain shape $W_{grain} = 1$, and the grain orientation $\theta_{grain} = 0^\circ$.

Table 1. Value of the material parameters of the constitutive model, typical for Al alloys.
– σ_0/E is the ratio of yield stress on Young's modulus, ν is the Poisson ratio, n is the strain hardening exponent, f_0 is the initial void volume fraction, W_0 is the initial void shape, and λ_0 is the initial void distribution parameter.

grain	σ_{0g}/E_g	ν_g	n_g	f_{0g}	W_{0g}	λ_{0g}
interior	10^{-3}	0.35	0.05	5×10^{-3}	1	1
GB layer	σ_{0p}/E_p	ν_p	n_p	f_{0p}	W_{0p}	λ_{0p}
	2 to 10	0.35	0.3	5×10^{-2} to 6×10^{-3}	1/3	1

3. Selected results and discussion

3.1 Single grain model (Model 2)

Fig. 3 shows stress-strain curves predicted with Model 2 for different yield stress ratios, using the parameters of Table 1. The transition from an intergranular fracture mode when the grain is much harder than the GB layer to transgranular fracture when the hardness mismatch gets smaller is clearly captured. Fig. 4 presents failure maps dividing the space defined by the applied stress ratio and the coverage of the GB (distance between particles L_{p0} divided by their diameter D_{p0}) into inter- and transgranular fracture regions. Intergranular fracture is promoted by a large stress triaxiality, low GB coverage as well as high yield stress ratio.

Note that the predictions of the bilayer model (Model 1) [4] agree qualitatively well with the single grain model (Model 2). Quantitatively, the presence of inclined GBs tends to relax the constraint in the soft layers, favouring slightly more the transgranular failure mode.

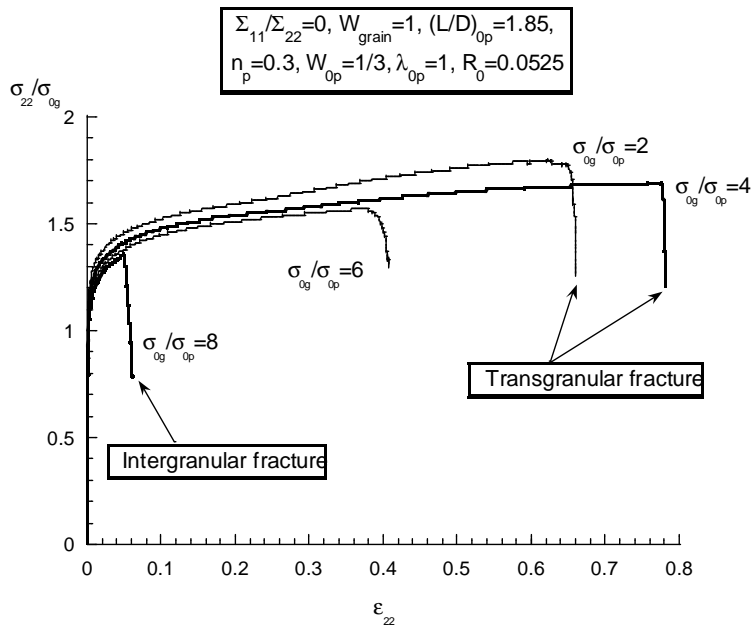


Fig. 3 Stress strain curves predicted with the single grain model (Model 2) for different ratios of yield stress between the grain interior and GB layer.

3.2 Multigrain model under homogenous loading conditions (Model 3)

Fig. 5 shows the variation obtained with three different grain distributions of the fracture strain as a function of yield stress mismatch for different applied stress ratios. Two distributions correspond to two different Voronoi tessellations (see Fig. 6 where the multigrain is embedded in a tensile sample) and one distribution is a perfect arrangement of identical hexagonal grains (equivalent to the single

grain model). The results found with the two statistical distributions are almost identical (i.e. the number of grains is sufficient so that statistical differences are averaged out), and the ductility is significantly smaller than for the perfect hexagonal arrangement, especially in the intergranular regime. The statistical distribution leads to weak crack paths, absent in the hexagonal distribution.

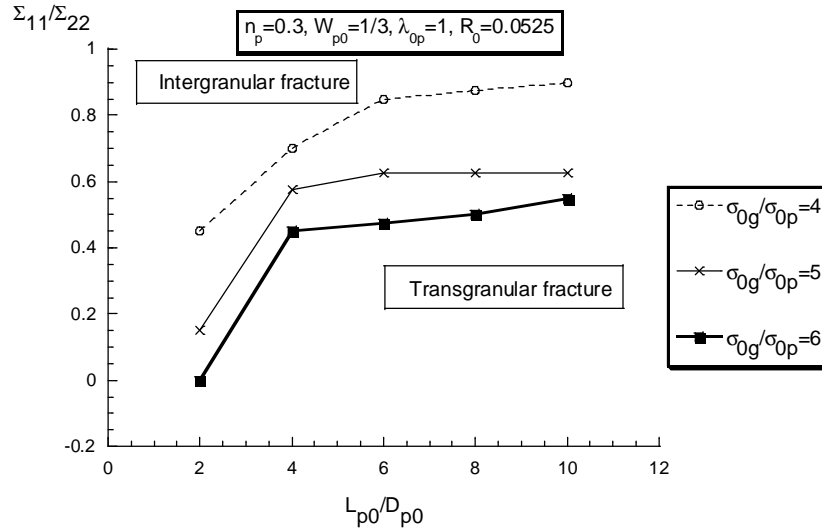


Fig. 4 Failure maps showing the regions of transgranular versus intergranular fracture as a function of applied stress ratio and GB coverage by second phase particles.

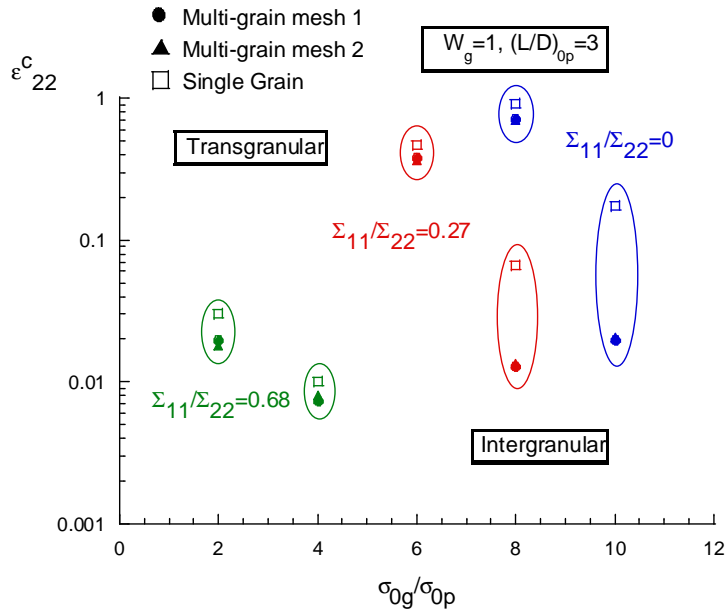


Fig. 5 Variation of the fracture strain as a function of the yield stress mismatch for different applied stress ratio and the three different grain arrangements shown in Fig. 6.

3.3 Uniaxial tension with necking

At the right of Fig. 6, a zoom is shown of the necking region of samples loaded up to fracture, for the three different grain distributions depicted in Fig. 6(a)-(c). Results are provided for both low yield stress mismatch (left column of snapshots) leading to significant amount of necking before transgranular failure and large yield stress mismatch (right column of snapshots) leading to small amounts of necking before intergranular failure. Again, a regular arrangement of grains provides an artificially high ductility. Transgranular failure shows evidence of cup and cone fracture combining flat and shear type cracking (especially with regular distribution), while intergranular fracture lead to relatively flat fracture surfaces.

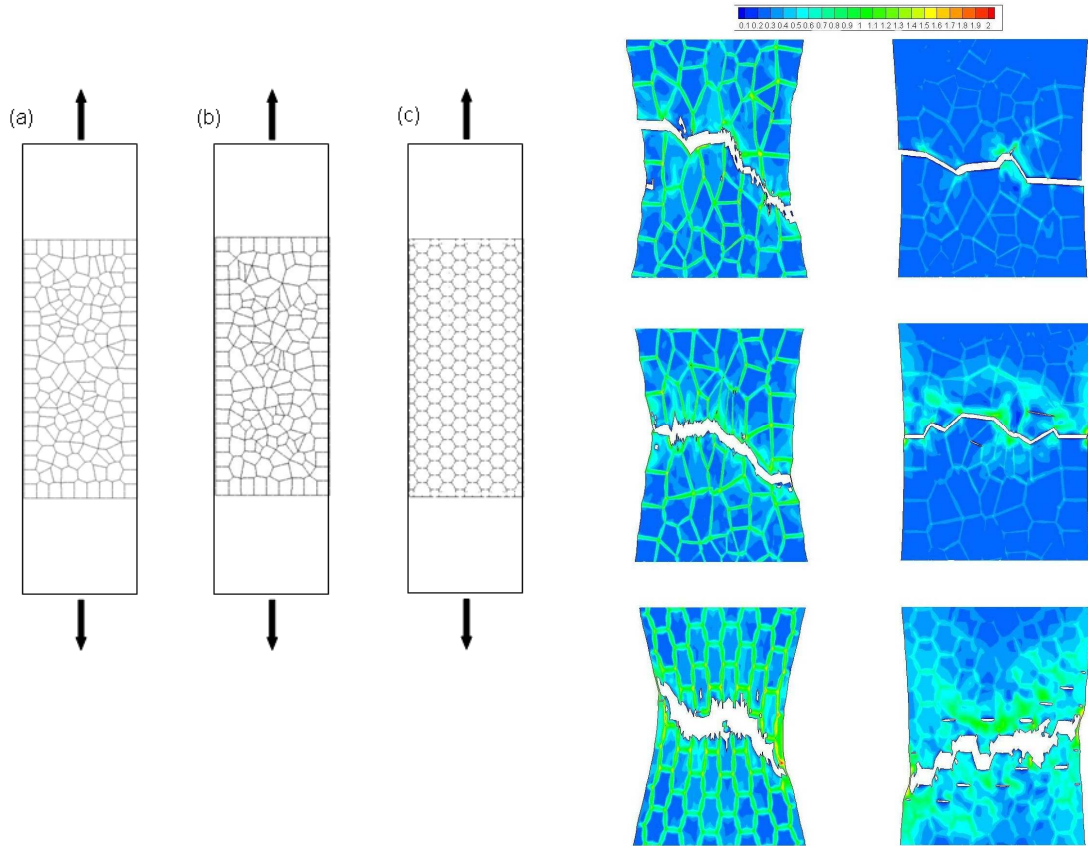


Fig. 6. Initial and final (fractured) configuration of tensile test samples for three different grain arrangements. The simulations are performed for a low (left column) and high (right column) yield stress mismatch leading to a transgranular large ductility failure and intergranular low ductility failure, respectively.

3.4 SSY multigrain model

Fig. 7 presents the J_R curves predicted with the SSY model for different yield stress mismatches. The effect of moving from intergranular to transgranular fracture is enormous in terms of tearing modulus. The crack profiles obtained for

one low and one high yield stress mismatch demonstrate that intergranular fracture involve, as expected, small crack tip blunting and relatively straight crack path along the weak grain boundary layers.

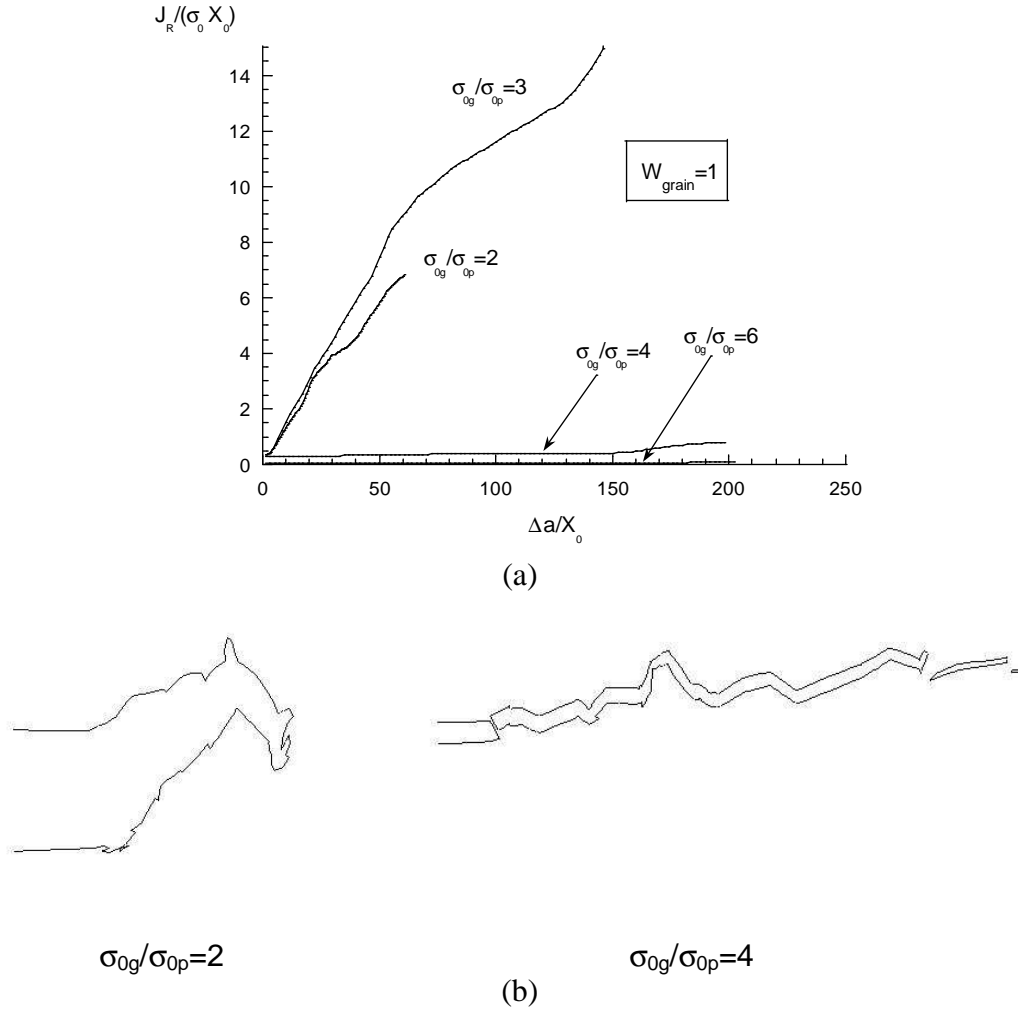


Fig. 7. Predictions obtained with SSY model in terms of (a) JR curves for different yield stress ratio and (b) crack profile for a low and high yield stress mismatch corresponding to transgranular and intergranular fracture modes, respectively.

4. Conclusions

The potential of an advanced micromechanics based computational model to simulate the damage evolution and fracture competition in heterogeneous alloys presenting soft GB layers has been demonstrated for different descriptions of the microstructure and loading conditions. On top of the yield stress mismatch, GB coverage and stress state addressed in this paper, other important physical parameters include grain shape, grain orientation, strain hardening capacity, and

GB layer thickness. An important extension of this study is also to link the result of thermal treatment to microstructure changes, based on which the present approach can be used to link process parameters to fracture properties.

5. Acknowledgements

Fruitful discussions about the present study with J.-B. Leblond and G. Perrin are gratefully acknowledged. FS acknowledges the support of the Walloon Region (DGTRE) and the Fonds Social Européen through a ‘‘FIRST EUROPE Objectif 3’’ project under the contract EPH3310300R0302/215284. This research was carried out under the University Attraction Poles (IAP) Programme, financed by the Belgian Science Policy under contract P6/24.

6. References

- [1] D. Dumont, A. Deschamps, Y. Bréchet, A model for predicting fracture mode and toughness in 7000 series aluminium alloys, *Acta Mater* 52 (2004) 2529–2540
- [2] T.F. Morgeneyer, M.J. Starink, S.C. Wang, I. Sinclair, Quench sensitivity of toughness in an Al alloy: Direct observation and analysis of failure initiation at the precipitate-free zone, *Acta Mater* 56 (2008) 2872–2884
- [3] T. Krol, D. Baither, E. Nembach, The formation of precipitate free zones along grain boundaries in a superalloy and the ensuing effects on its plastic deformation, *Acta Mater* 52 (2004) 2095–2108
- [4] T. Pardoën, D. Dumont, A. Deschamps, Y. Bréchet, Grain boundary versus transgranular ductile failure, *J Mech Phys Solids* 51 (2003) 637–665
- [5] M. Gologanu, J.-B. Leblond, G. Perrin, J. Devaux, Recent extensions of Gurson’s model for porous ductile metals, in: P. Suquet (Ed.), *Continuum Micromechanics, CISM Lectures Series*, Springer, New York, 1997, pp. 61–130
- [6] A. Gurson, Continuum theory of ductile rupture by void nucleation and growth: Part I— Yield criteria and flow rules for porous ductile media, *J Eng Mater Technol* 99 (1977) 2–15
- [7] M. Kaisalam, P. Ponte Castañeda, A general constitutive theory for linear and nonlinear particulate media with microstructure evolution, *J Mech Phys Solids* 46 (1998) 427–465
- [8] P.F. Thomason, *Ductile Fracture of Metals*, Pergamon Press, Oxford, 1990
- [9] F. Scheyvaerts., P. Onck, Y. Bréchet, T. Pardoën, A new model for void coalescence by internal necking. *Int J Damage Mech*, in press
- [10] T. Pardoën, J.W. Hutchinson, 2000, An extended model for void growth and coalescence, *J Mech Phys Solids* 48 (2000) 2467–2512
- [11] F. Scheyvaerts, P.R. Onck, T. Pardoën, The growth and coalescence of voids under combined shear and tension, submitted to *J Mech Phys Solids*